Applied Soft Computing 46 (2016) 543–557

Contents lists available at ScienceDirect

Applied Soft Computing

journal homepage: www.elsevier.com/locate/asoc

An improved intuitionistic fuzzy c-means clustering algorithm incorporating local information for brain image segmentation

Hanuman Verma*, R.K. Agrawal, Aditi Sharan

School of Computer and Systems Sciences, Jawaharlal Nehru University, New Delhi, India

ARTICLE INFO

Article history:
Received 24 March 2015
Received in revised form 23 October 2015
Accepted 5 December 2015
Available online 23 December 2015

Keywords:
Intuitionistic fuzzy sets
Fuzzy c-means
Intuitionistic fuzzy c-means
Magnetic resonance imaging
Image segmentation

ABSTRACT

The segmentation of brain magnetic resonance (MR) images plays an important role in the computer-aided diagnosis and clinical research. However, due to presence of noise and uncertainty on the boundary between different tissues in the brain image, the segmentation of brain image is a challenging task. Many variants of standard fuzzy c-means (FCM) algorithm have been proposed to handle the noise. Intuitionistic fuzzy c-means (IFCM) algorithm, one of the variants of FCM, is found suitable for image segmentation. It incorporates the advantage of intuitionistic fuzzy sets theory. The IFCM successfully handles the uncertainty but it is sensitive to noise as it does not incorporate any local spatial information. In this paper, we have presented a novel approach, named an improved intuitionistic fuzzy c-means (IIFCM), which considers the local spatial information in an intuitionistic fuzzy way. The IIFCM preserves the image details, is insensitive to noise, and is free of requirement of any parameter tuning. The obtained segmentation results on synthetic square image, real and simulated MRI brain image demonstrate the efficacy of the IIFCM algorithm and superior performance in comparison to existing segmentation methods. A nonparametric statistical analysis is also carried out to show the significant performance of the IIFCM algorithm in comparison to other existing segmentation algorithms.

1. Introduction

The segmentation of human brain image from magnetic resonance imaging (MRI) into three brain tissues: cerebrospinal fluid (CSF), gray matter (GM) and white matter (WM) [1] is one of the important components in computer-aided diagnosis and neuroscience research. It helps to detect different diseases such as tumors, edema [2], Alzheimer's Disease (AD) [3] and Schizophrenia [4]. Due to complicated structure of human brain and absence of well-defined boundary between different tissues, segmentation of brain image is a very difficult task. In literature, various segmentation methods such as thresholding based methods [5], atlas-guided methods [6], artificial neural network (ANN) [7], Markov random field model [8], level set methods [9], and clustering methods [10,11] etc. have been suggested for MRI. Thresholding based method is used when the histograms of different brain tissues namely, GM, WM and CSF are quite distinguishable. Due to complex distribution of intensities of different brain tissues, the determination of appropriate threshold for brain image segmentation is difficult. Atlas-guided method [6] finds a transformation to map a pre-segmented atlas image to the target image that requires to be segmented. However, atlas-based method has a limitation due to the anatomical variability exhibited in the available atlases which does not explicitly model the intensity of the given new image. Artificial neural network (ANN) is a machine learning model in which the learning is achieved by updating the weight assigned to the connection between the different nodes. Due to many interconnections between the different nodes, the ANN model incorporates the spatial information during the segmentation. The Markov random field (MRF) model is itself not a segmentation method but a statistical model which can be used within other segmentation methods. Various segmentation algorithms have used the MRF model to incorporate the spatial information that occurs in the neighboring pixels. The level set method [9] is a non-parametric approach to track shapes and interfaces. It determines contours/surfaces with well-established mathematical theories such as calculus of variations and partial differential equations. Clustering methods are considered to be efficient for MRI brain image segmentation. The basic idea of clustering is to group similar pixels. In literature, various clustering methods such as Expectation-maximization [10], k-means [11] and fuzzy clustering methods [12] have been suggested. The k-means algorithm performs segmentation of the image which involves iterative computation of mean intensity for

* Corresponding author.
E-mail addresses: hv4231@gmail.com (H. Verma), rkajnu@gmail.com (R.K. Agrawal), aditisharan@mail.jnu.ac.in (A. Sharan).

http://dx.doi.org/10.1016/j.asoc.2015.12.022
1568-4946/

each cluster and assigning each pixel to the cluster whose mean is closest to the particular pixel. In the EM algorithm, it is assumed that the data follows a Gaussian mixture model. It iterates to determine the posterior probabilities, maximum likelihood estimates of the means, covariances, and mixing parameters of the mixture model to perform clustering. However, it is found to be sensitive to the choice of initial parameters. Among these clustering approaches, the standard fuzzy c-means (FCM) algorithm [12] and its variants are widely used by image and pattern recognition research community. The FCM works well for noiseless images. But, one major disadvantage of the standard FCM algorithm during segmentation is that it does not consider any spatial information [13–15], which makes it sensitive to noise.

In literature, many researchers have attempted to incorporate the local spatial information in the standard FCM algorithm. Pham [14] introduced the robust fuzzy c-means (RFCM) algorithm with modification of the standard FCM objective function, which includes the local spatial penalty term. This penalty term allows computation of the smooth membership function. It improves the segmentation performance and is insensitive of noise to some extent. Another approach, the fuzzy clustering with spatial constraints (FCM_S) proposed by Ahmed et al. [16], overcomes the problem of the intensity inhomogeneity. This is achieved by adding a term in the objective function of the standard FCM which allows smoothing of pixels by its neighborhood pixels. The FCM_S algorithm is insensitive to noise to some extent but it takes more execution time as it involves computation of neighborhood term in all iterations during clustering process. To reduce the execution time of the FCM_S algorithm, Chen and Zhang [17] suggested two variants of FCM_S algorithm, named the FCM_S1 and FCM_S2 algorithms. The mean filtered image is computed in the FCM_S1 whereas median filtered image is computed in FCM_S2 algorithm in advance, to replace the neighborhood term of the FCM_S algorithm. Shen et al. [2] pointed that RFCM, FCM_S, FCM_S1 and FCM_S2 algorithms loses the continuity from the standard FCM, as these algorithms are formulated with modification of standard FCM objective function. Further, Shen et al. [2] suggested a new algorithm, named improved fuzzy c-means (ImFCM) by introducing the neighborhood attraction term in its distance measure. This neighborhood attraction depends on two factors; one is pixel intensities and other is spatial position of the surrounding pixels. The ImFCM uses two parameters β and ψ whose optimal values are learned using artificial neural network model to adjust the degree of two factors in the neighborhood attraction [2]. However it requires additional execution time to learn parameters using artificial neural network model. Szilagyi et al. [18] suggested the enhanced fuzzy c-means (EnFCM) which is faster. In the EnFCM algorithm, the clustering is carried out on the gray-level histogram of newly generated image, which is obtained from the original image and its local neighbor average image. Generally, in an image, total number of gray-levels is less in comparison to the total number of pixels and this reduces significantly the execution time of EnFCM algorithm. Another similar research work is suggested by Cai et al. [19], the fast generalized fuzzy c-means (FGFCM), which incorporates both local spatial and gray-level information by introducing a similarity measure factor. To incorporate the local spatial information in the standard FCM, Krinidis and Chatzis [20] suggested fuzzy local information c-means (FLICM) algorithm by including a new fuzzy local neighborhood factor in the objective function of standard FCM algorithm. The new fuzzy local neighborhood factor determines gray-level and spatial relationship and does not require any parameter setting.

In addition to sensitivity to noise, another major challenge in segmentation of brain image is to handle the uncertainty that arises on boundary between different tissues. To handle this type of uncertainty, Atanassov [21] suggested the generalization of fuzzy sets theory, known as intuitionistic fuzzy sets (IFS) theory. To exploit the advantage of IFS theory, Pelekis et al. [22] proposed the fuzzy clustering of intuitionistic fuzzy data, where the qualitative information, which is obtained via intuitionistic membership μ_p and non-membership degree ν_p for each data point x_p is used. The n-dimensional data point x_p represented in IFS theory is a vector of triplet i.e. $[(x_{p_1}, \mu_{p_1}, \nu_{p_1}), (x_{p_2}, \mu_{p_2}, \nu_{p_2}), \ldots, (x_{p_n}, \mu_{p_n}, \nu_{p_n})]$ instead of vector $(x_{p_1}, x_{p_2}, \ldots, x_{p_n})$ in fuzzy set theory. Xu and Wu [23] suggested the intuitionistic fuzzy c-means (IFCM) algorithm which utilizes the intuitionistic fuzzy distance instead of fuzzy distance. The IFCM successfully handles the uncertainty but one main shortcoming of the IFCM algorithm is that it does not include any local spatial information, which makes its susceptible to noise.

To make IFCM insensitive to noise, we present a new algorithm, named an improved intuitionistic fuzzy c-means (IIFCM), which incorporates the local spatial information in IFCM by introducing a new intuitionistic fuzzy factor. This factor determines both local gray-level and spatial information and is free of any parameter tuning. The IIFCM has following characteristics: (i) the intuitionistic fuzzy factor in the IIFCM incorporates simultaneous both local gray-level and local spatial information; (ii) the balance between image details and noise are automatically maintained by intuitionistic fuzzy local constraints; (iii) no need of pre-processing step to apply the IIFCM; (iv) it utilizes qualitative information which is obtained via intuitionistic fuzzy membership μ_p, non-membership ν_p for the given data point x_p. The proposed IIFCM algorithm is tested on a synthetic square image and brain images of two publically available brain databases. To check the efficacy of the proposed approach (IIFCM), the performance is evaluated in the terms of similarity index, false negative ratio and false positive ratio, and compared quantitatively with seven existing segmentation methods. A non-parametric statistical test based on multiple comparisons with a control method is also carried out to compare the performance of segmentation algorithms.

The rest part of the paper is structured as follows. Section 2 describes IFS theory, similarity measure and intuitionistic fuzzification of images. Section 3, briefly describes FCM_S, FCM_S1, FCM_S2, EnFCM, FGFCM, FLICM and IFCM algorithms. The proposed IIFCM algorithm is described in Section 4. Experimental results and comparison with seven exiting algorithms are included in Section 5. Finally, Section 6 includes the conclusions.

2. Intuitionistic fuzzy sets, similarity measure and intuitionistic fuzzification of images

In this section, we describe briefly intuitionistic fuzzy sets, similarity measures between elements and intuitionistic fuzzification of images.

2.1. Intuitionistic fuzzy sets

Zadeh [24] defined the fuzzy set $A = \{\langle x, \mu_A(x)\rangle : \forall x \in X\}$ on the set $X = \{x_1, x_2, \ldots, x_N\}$, where $\mu_A : X \to [0, 1]$ denotes the membership degree for each $x \in X$. The non-membership degree ν_A of fuzzy set A is defined as $\nu_A = 1 - \mu_A$. But, in real situations, while defining the membership degree another uncertainty (hesitation) arises. To handle this type of uncertainty, Atanassov [21] proposed the intuitionistic fuzzy sets (IFS) theory. The IFS B on the set X is defined by Atanassov as [21]:

$$B = \{\langle x, \mu_B(x), \nu_B(x)\rangle : \forall x \in X\} \quad (1)$$

where $\mu_B : X \to [0, 1]$ denote the membership and $\nu_B : X \to [0, 1]$ denote the non-membership degree for each $x \in X$ of the set $B \subseteq X$

and it holds the condition $0 \le \mu_B(x) + \nu_B(x) \le 1$. The function defined as [21]

$$\pi_B(x) = 1 - \mu_B(x) - \nu_B(x) \tag{2}$$

is called hesitation degree for each $x \in X$. It is evident that $0 \le \pi_B \le 1$ for each $x \in X$.

In literature, Sugeno [25] and Yager [26,27] suggested negation function to determine the non-membership degree ν_B for construction of intuitionistic fuzzy set. The Sugeno's negation function is defined [25] as:

$$N(x) = \frac{1-x}{1+\lambda x} \quad \lambda > 0 \tag{3}$$

Using Sugeno's negation function, the IFS B defined in Eq. (1) can be rewritten as:

$$B = \left\{ \left\langle x, \mu_B(x), \nu_B(x) = \frac{1-\mu_B(x)}{1+\lambda(\mu_B(x))} \right\rangle : \forall x \in X \right\} \tag{4}$$

2.2. Similarity measure between elements

The similarity measure [28] between two objects measures the degree of similarity. Let $IFS(X)$ be the set of all intuitionistic fuzzy sets on the set X. A function $s : IFS(X) \times IFS(X) \to [0, 1]$ measures the similarity between two IFS C and D in $IFS(X)$, has the following properties [28]:

$$0 \le s(C, D) \le 1; \tag{P1}$$

$$s(C, D) = 1 \quad \text{iff } C = D; \tag{P2}$$

$$s(C, D) = s(D, C); \tag{P3}$$

$$\text{If } s(C, D) = 0 \text{ and } s(C, E) = 0, E \in IFS(X), \text{ then } s(D, E) = 0 \tag{P4}$$

If C and D are two intuitionistic fuzzy sets in $IFS(X)$, where $C = \{\langle x, \mu_C(x), \nu_C(x)\rangle : \forall x \in X\}$ and $D = \{\langle x, \mu_D(x), \nu_D(x)\rangle : \forall x \in X\}$, then similarity measure $s(C, D)$ between two intuitionistic fuzzy sets C and D in $IFS(X)$ is defined [28] as:

$$s(C, D) = \frac{\sum_{l=1}^{N} \mu_C(x_l)\mu_D(x_l) + \nu_C(x_l)\nu_D(x_l) + \pi_C(x_l)\pi_D(x_l)}{\max\left(\sum_{l=1}^{N}((\mu_C(x_l))^2 + (\nu_C(x_l))^2 + (\pi_C(x_l))^2), \sum_{l=1}^{N}((\mu_D(x_l))^2 + (\nu_D(x_l))^2 + (\pi_D(x_l))^2)\right)} \tag{5}$$

In literature Hyung et al. [29] and Wang [30] introduced the definition of the similarity measure on fuzzy sets and on elements. Liu [31] introduced the new definition of similarity measures between intuitionistic fuzzy sets and between elements. Let $D_k (k = 1, 2, 3, \ldots, c)$ denote the IFS on the set X, where $D_k = \{\langle x_i, \mu_{D_k}(x_i), \nu_{D_k}(x_i)\rangle : \forall x_i \in X\}$. The function s_e measures the similarity between two elements $x_i, x_j \in X$ in IFS D_k, which has the following properties [31]:

$$0 \le s_e(x_i, x_j) \le 1; \tag{p1}$$

$$s_e(x_i, x_j) = 1 \quad \text{iff } \mu_{D_k}(x_i) = \mu_{D_k}(x_j), \quad \nu_{D_k}(x_i) = \nu_{D_k}(x_j); \tag{p2}$$

$$s_e(x_i, x_j) = s_e(x_j, x_i). \tag{p3}$$

Using Eq. (5), the similarity measure between two elements x_i, $x_j \in X$ in IFS D_k is defined as:

$$s_e(x_i, x_j) = \frac{\sum_{k=1}^{c} \mu_{D_k}(x_i)\mu_{D_k}(x_j) + \nu_{D_k}(x_i)\nu_{D_k}(x_j) + \pi_{D_k}(x_i)\pi_{D_k}(x_j)}{\max\left(\sum_{k=1}^{c}((\mu_{D_k}(x_i))^2 + (\nu_{D_k}(x_i))^2 + (\pi_{D_k}(x_i))^2), \sum_{k=1}^{c}((\mu_{D_k}(x_j))^2 + (\nu_{D_k}(x_j))^2 + (\pi_{D_k}(x_j))^2)\right)} \tag{6}$$

Above Eq. (6) satisfies the given properties (p1)–(p3). It is obvious that Eq. (6) also satisfies the property (p4) for two elements x_i, $x_j \in X$ in IFS D_k as follows:

$$\text{If } s_e(x_i, x_j) = 0 \text{ and } s_e(x_j, x_m) = 0, x_m \in X, \text{ then } s_e(x_i, x_m) = 0 \tag{p4}$$

2.3. Intuitionistic fuzzification of images

The intuitionistic fuzzy clustering algorithm requires intuitionistic fuzzy data. Vlachos and Sergiadis [32] suggested the representation of image in terms of IFS, which is defined as follows. Let B be an image of size $P \times Q$ with $N(= PQ)$ pixels, which are having L gray levels values between the range 0 and $L-1$. The image B in terms of IFS is represented as:

$$B = \{\langle x_j, \mu_B(x_j), \nu_B(x_j)\rangle : j = 1, 2, \ldots, N\} \tag{7}$$

where $\mu_B(x_j)$ and $\nu_B(x_j)$ denote the membership and non-membership degree of the pixels x_j respectively. The membership degree of each pixel x_j of an image in terms of normalized intensity level is given as follows:

$$\mu_B(x_j) = \frac{x_j - (x_j)_{\min}}{(x_j)_{\max} - (x_j)_{\min}}, \quad j = 1, 2, \ldots, N, \quad x_j \in \{0, \ldots, L-1\} \tag{8}$$

where $(x_j)_{\max}$ and $(x_j)_{\min}$ denote the maximum and minimum gray level values of the image respectively.

3. Related works

3.1. Fuzzy clustering with constraints (FCM_S) and its variants

The fuzzy clustering with constraints (FCM_S) algorithm proposed by Ahmed et al. [16] includes a penalty term in the standard FCM objective function. This penalty term allows the smoothing of a pixel within its specified neighborhood. The optimization problem of the FCM_S algorithm [16] is given as:

$$\begin{cases} \min\ J_m(\mathbf{U}, \mathbf{V} : \mathbf{X}) = \sum_{i=1}^{c}\sum_{j=1}^{N}(u_{ij})^m \left\|x_j - v_i\right\|^2 + \frac{\alpha}{N_R}\sum_{i=1}^{c}\sum_{j=1}^{N}(u_{ij})^m \sum_{r \in N_j}\|x_r - v_i\|^2 \\ \text{subject to } \sum_{i=1}^{c} u_{ij} = 1, 1 \le j \le N \end{cases} \tag{9}$$

where $\mathbf{X} = \{x_1, x_2, \ldots, x_N\}$ are N pixels, $m\,(1 < m < \infty)$ is the fuzzifier constant, $c\,(1 < c < N)$ is the number of clusters which are fixed, $\mathbf{V} = (v_1, v_2, \ldots, v_c)$ denotes the centroids of clusters, $u_{ij} (0 \le u_{ij} \le 1)$ denote the membership degree, $\mathbf{U} = (u_{ij})_{c \times N}$ is membership matrix, N_j represent the number of neighboring pixels around the centered pixel x_j, N_R denotes the cardinality of N_j and parameter α controls the tradeoff effects of the neighboring term. The membership matrix $\mathbf{U}$ also satisfies the condition $0 < \sum_{j=1}^{N} u_{ij} < N$, $\forall i$. The optimization problem (9) can be solved by Lagrangian multiplier method, and its membership and centroids are given [16] as:

$$u_{ij}=\frac{\left(\left\|x_j-v_i\right\|^2+\frac{\alpha}{N_R}\sum_{r\in N_j}\|x_r-v_i\|^2\right)^{-1/(m-1)}}{\sum_{k=1}^{c}\left(\left\|x_j-v_k\right\|^2+\frac{\alpha}{N_R}\sum_{r\in N_j}\|x_r-v_k\|^2\right)^{-1/(m-1)}},\quad 1\le i\le c,\quad 1\le j\le N \tag{10}$$

$$v_i=\frac{\sum_{j=1}^{N}u_{ij}^m\left(x_j+\frac{\alpha}{N_R}\sum_{r\in N_j}x_r\right)}{(1+\alpha)\sum_{j=1}^{N}u_{ij}^m},\quad 1\le i\le c \tag{11}$$

Term $\frac{1}{N_R}\sum_{r\in N_j}x_r$ in Eq. (11) represents the average value of gray-level around the pixel x_j within the specified window. The mean filtered image is composed of its neighbor average gray values around each pixel within a window.

However, the execution time of the FCM_S algorithm is high. In order to reduce the execution time of the FCM_S algorithm, a variant of FCM_S algorithm, named the FCM_S1 is introduced by Chen and Zhang [17], with modification of the objective function of the FCM_S. The optimization problem of the FCM_S1 is given as:

$$\begin{cases}\min J_m(\mathbf{U},\mathbf{V}:\mathbf{X})=\sum_{i=1}^{c}\sum_{j=1}^{N}(u_{ij})^m\left\|x_j-v_i\right\|^2+\alpha\sum_{i=1}^{c}\sum_{j=1}^{N}(u_{ij})^m\left\|\bar{x}_j-v_i\right\|^2\\ \text{subject to}\sum_{i=1}^{c}u_{ij}=1,\ 1\le j\le N\end{cases} \tag{12}$$

where $\bar{x}_j$ is the mean value of neighboring pixels around the pixel x_j and this mean value is computed in advance. The optimization problem (12) can be solved by Lagrangian multiplier method, and its membership and centroids are obtained [17] as:

$$u_{ij}=\frac{\left(\left\|x_j-v_i\right\|^2+\alpha\left\|\bar{x}_j-v_i\right\|^2\right)^{-1/(m-1)}}{\sum_{k=1}^{c}\left(\left\|x_j-v_k\right\|^2+\alpha\left\|\bar{x}_j-v_k\right\|^2\right)^{-1/(m-1)}},\quad 1\le i\le c,\quad 1\le j\le N \tag{13}$$

$$v_i=\frac{\sum_{j=1}^{N}u_{ij}^m(x_j+\alpha\bar{x}_j)}{(1+\alpha)\sum_{j=1}^{N}u_{ij}^m},\quad 1\le i\le c \tag{14}$$

Further, to achieve the more robustness, another variant of the FCM_S algorithm, named the FCM_S2 suggested by Chen and Zhang [17]. In FCM_S2, median-filtered image is used instead of the mean-filtered image used in FCM_S1 algorithm. Both FCM_S1 and FCM_S2 algorithms simplify the neighborhood term of the FCM_S algorithm and are suitable for digital image which is contaminated by Gaussian and impulsive noise respectively. The parameter α controls the tradeoff effect between the filtered (mean or median) image and original image. If the parameter α is set to zero, then FCM_S, FCM_S1 and FCM_S2 reduce to the FCM algorithm. The outline of FCM_S1 and FCM_S2 algorithms are depicted [17] as:

Algorithm 1. FCM_S1 Algorithms

Step 1: Set the number of clusters c, fuzzifier constant m and stopping criterion ε
Step 2: Compute in advance the mean filtered image
Step 3: Initialize the membership degree $\mathbf{U}^{(0)}$ with setting the loop counter $a=0$
Step 4: Compute the centroids $v_i^{(a)}$ using Eq. (14) for FCM_S1
Step 5: Compute the membership degrees $\mathbf{U}^{(a+1)}$ using Eq. (13) for FCM_S1
Step 6: Stop if max $\left\|\mathbf{U}^{(a+1)}-\mathbf{U}^{(a)}\right\|<\varepsilon$, otherwise set counter $a=a+1$ and go to step 4

Algorithm 2. FCM_S2 Algorithms

Step 1: Set the number of clusters c, fuzzifier constant m and stopping criterion ε
Step 2: Compute in advance the median filtered image
Step 3: Initialize the membership degree $\mathbf{U}^{(0)}$ with setting the loop counter $a=0$
Step 4: Compute the centroids $v_i^{(a)}$ using Eq. (14) for FCM_S2
Step 5: Compute the membership degrees $\mathbf{U}^{(a+1)}$ using Eq. (13) for FCM_S2
Step 6: Stop if max $\left\|\mathbf{U}^{(a+1)}-\mathbf{U}^{(a)}\right\|<\varepsilon$, otherwise set counter $a=a+1$ and go to step 4

3.2. Enhanced fuzzy c-means algorithm

In order to reduce the execution time during segmentation of MRI brain images, Szilagyi et al. [18] introduced a new algorithm, named the Enhanced fuzzy c-means (EnFCM). In EnFCM algorithm, firstly, a linearly-weighted image ξ is obtained from the existing original image, which is defined in terms of local neighbors [18] as:

$$\xi_j=\frac{1}{1+\alpha}\left(x_j+\frac{\alpha}{N_R}\sum_{r\in N_j}x_r\right),\quad 1\le j\le N \tag{15}$$

where ξ_j represent the gray level value of jth pixel of the new image ξ, N_j represents the number of neighboring pixels around the centered pixel x_j, N_R denotes the cardinality of N_j and parameter α controls the tradeoff effects of the neighboring term. The EnFCM algorithm is performed on the gray-level histogram of the image ξ. The optimization problem for the EnFCM is formulated [18] as:

$$\begin{cases}\min J_m(\mathbf{U},\mathbf{V}:\boldsymbol{\xi})=\sum_{i=1}^{c}\sum_{l=1}^{q}\gamma_l(u_{il})^m(\xi_l-v_i)^2\\ \text{subject to}\sum_{i=1}^{c}u_{il}=1,\quad 1\le l\le q\end{cases} \tag{16}$$

where q denotes the number of gray levels of image, $m\,(1<m<\infty)$ is the fuzzifier constant, $c\,(1<c<q)$ is the number of clusters, $\mathbf{V}=(v_1,v_2,\ldots,v_c)$ denotes the centroids of clusters, $u_{il}(0\le u_{il}\le 1)$ is the membership degree of lth gray-level value to the ith cluster center and q is the total number of gray-level of the original image which is very small in comparison to N. The γ_l represents number of pixels with the gray-level value equal to l and it satisfies the condition $\sum_{l=1}^{q}\gamma_l=N$. Using Lagrangian multiplier method, the non-linear problem (16) can be solved, and its membership and centroids are given [18] as:

$$u_{il}=\frac{(\xi_l-v_i)^{-2/(m-1)}}{\sum_{k=1}^{c}(\xi_l-v_k)^{-2/(m-1)}},\quad 1\le i\le c,\quad 1\le l\le q \tag{17}$$

$$v_i=\frac{\sum_{l=1}^{q}\gamma_l u_{il}^m\xi_l}{\sum_{l=1}^{q}\gamma_l u_{il}^m},\quad 1\le i\le c \tag{18}$$

The outline of the EnFCM algorithm is given [18] as follows:

Algorithm 3. Enhanced fuzzy c-means (EnFCM) algorithm

Step 1: Set the number of clusters c, fuzzifier constant m and stopping criterion ε
Step 2: Compute the linearly-weighted sum image ξ using Eq. (15)
Step 3: Initialize the membership degree $U^{(0)}$ with setting the loop counter $a = 0$
Step 4: Compute the centroids $v_i^{(a)}$ using Eq. (18)
Step 5: Compute the membership degrees $\mathbf{U}^{(a+1)}$ using Eq. (17)
Step 6: Stop if max $\left\|\mathbf{U}^{(a+1)} - \mathbf{U}^{(a)}\right\| < \varepsilon$, otherwise set counter $a = a + 1$ and go to step 4

The computation time of EnFCM algorithm is reduced significantly and provides segmentation results comparable to the FCM_S algorithm. The segmentation performance depends on the choice of parameter α and window size. If the value of parameter α is large, then it is more resistant to noise [17] and if it is chosen small then segmentation result maintains the sharpness and details of the image. Hence, the selection of optimal value of parameter α is a difficult task.

3.3. Fast generalized fuzzy c-means algorithm

In order to improve the robustness of clustering algorithms, Cai et al. [19] introduced the fast generalized fuzzy c-means (FGFCM) algorithm. The FGFCM algorithm exploits the local spatial information by introducing the local similarity measure S_{ij}, which is defined [19] as:

$$S_{ij} = \begin{cases} \exp(-\max(|p_i - p_j|, |q_i - q_j|)/\lambda_s - \left\|x_i - x_j\right\|^2/(\lambda_g \sigma_j^2)) & i \neq j \\ 0 & i = j \end{cases} \tag{19}$$

where S_{ij} denotes the local similarity measure of the ith and jth pixels and the ith pixel are the number of neighboring pixels around the centered jth pixel. The terms (p_j, q_j) and x_j denote the two dimensional spatial coordinate and gray-level value of the jth pixel respectively. The parameters λ_s and λ_g denote the scale factors of the spread of local spatial and gray-level relationship respectively. The value of λ_s is fixed to 3 according to the research work [19] and optimal value of λ_g is used. The parameter σ_j is calculated as [19]:

$$\sigma_j = \sqrt{\frac{\sum_{i \in N_j} \left\|x_i - x_j\right\|^2}{N_R}}, \quad 1 \leq j \leq N \tag{20}$$

where N_j represents the number of neighboring pixels around the centered pixel x_j and N_R denotes the cardinality of N_j. Using the factor S_{ij}, the newly generated image ξ is computed [19] as:

$$\xi_j = \frac{\sum_{i \in N_j} S_{ij} x_i}{\sum_{i \in N_j} S_{ij}}, \quad 1 \leq j \leq N \tag{21}$$

The only difference between the EnFCM and FGFCM algorithms is the process of determining the new image ξ_j. So, replacing the new image ξ_j (Eq. (15)) in the EnFCM algorithm with the new image ξ_j (Eq. (21)), the centroids and membership degree of the FGFCM algorithm are obtained. The outline of the FGFCM algorithm is given [19] as:

Algorithm 4. Fast generalized fuzzy c-means (FGFCM) algorithm

Step 1: Set the number of clusters c, fuzzifier constant m and stopping criterion ε
Step 2: Compute the local similarity measure S_{ij} using Eq. (19)
Step 3: Compute the linearly-weighted sum image ξ using Eq. (21)
Step 4: Initialize the membership degree $\mathbf{U}^{(0)}$ with setting the loop counter $a = 0$
Step 5: Compute the centroids $v_i^{(a)}$ using Eq. (18)
Step 6: Compute the membership degrees $\mathbf{U}^{(a+1)}$ using Eq. (17)
Step 7: Stop if max $\left\|\mathbf{U}^{(a+1)} - \mathbf{U}^{(a)}\right\| < \varepsilon$, otherwise set counter $a = a + 1$ and go to step 5

3.4. Fuzzy local information c-means algorithm

Fuzzy local information c-means (FLICM) algorithm is proposed by Krinidis and Chatzis [20] which includes a new factor G_{ij} in its optimization function. This new factor considers the local spatial information and controls the balance between the image details and image noise, and it does not requires any parameter tuning. The mathematical formulation of the FLICM algorithm is defined [20] as:

$$\begin{cases} \min J_m(\mathbf{U}, \mathbf{V} : \mathbf{X}) = \sum_{i=1}^{c} \sum_{j=1}^{N} (u_{ij})^m \left\|x_j - v_i\right\|^2 + G_{ij} \\ \text{subject to} \sum_{i=1}^{c} u_{ij} = 1, \quad 1 \leq j \leq N \end{cases} \tag{22}$$

where $\mathbf{X} = \{x_1, x_2, \ldots, x_N\}$ is set of N pixels, $m (1 < m < \infty)$ is the fuzzifier constant, $c (1 < c < N)$ is the number of clusters, $\mathbf{V} = (v_1, v_2, \ldots, v_c)$ denote the centroids of cluster, $u_{ij} (0 \leq u_{ij} \leq 1)$ is the membership degree and $\mathbf{U} = (u_{ij})_{c \times N}$ is the membership matrix. The term G_{ij} is called as fuzzy factor, which is defined [20] as:

$$G_{ij} = \sum_{\substack{k \in N_j \\ k \neq j}} \frac{1}{d_{jk} + 1} (1 - u_{ik})^m \left\|x_k - v_i\right\|^2, \quad 1 \leq i \leq c, \ 1 \leq j \leq N \tag{23}$$

where kth pixel is neighboring pixels around the centered jth pixel, N_j represents the number of neighboring pixels around the centered pixel x_j and d_{jk} is the spatial Euclidean distant between jth and kth pixels. The optimization problem (22) can be solved by Lagrangian multiplier method, and its membership degree u_{ij} and centroids v_i are given [20] as:

$$u_{ij} = \frac{1}{\sum_{r=1}^{c} \left(\frac{\left\|x_j - v_i\right\|^2 + G_{ij}}{\left\|x_j - v_r\right\|^2 + G_{rj}} \right)^{\frac{1}{m-1}}}, \quad 1 \leq i \leq c, \ 1 \leq j \leq N \tag{24}$$

$$v_i = \frac{\sum_{j=1}^{N} u_{ij}^m x_j}{\sum_{j=1}^{N} u_{ij}^m}, \quad 1 \leq i \leq c \tag{25}$$

The outline of the FLICM algorithm [20] is given as:

Algorithm 5. Fuzzy local information c-means (FLICM) algorithm

Step 1: Fixed the number of clusters c, fuzzifier constant m and termination criterion ε
Step 2: Initialize the membership degree $\mathbf{U}^{(0)}$ with setting the loop counter $a = 0$
Step 3: Compute the centroids $v_i^{(a)}$ using Eq. (25)
Step 4: Compute the fuzzy factor G_{ij} using Eq. (23)
Step 5: Compute the membership degree $\mathbf{U}^{(a+1)}$ using Eq. (24)
Step 6: Stop if max $\left\|\mathbf{U}^{(b+1)} - \mathbf{U}^{(b)}\right\| < \varepsilon$, otherwise set counter $a = a + 1$ and go to step 3

3.5. Intuitionistic fuzzy c-means algorithm

Xu and Wu [23] introduced intuitionistic fuzzy c-means (IFCM) algorithm which includes the advantage of intuitionistic fuzzy sets over the fuzzy sets in the FCM algorithm [12]. The IFCM gives better clusters and handles uncertainty that arises due to imprecise

information. The non-linear optimization problem of the IFCM is described [23] as:

$$\begin{cases} \min J_m(\mathbf{U}, \mathbf{V}^{IFS} : \mathbf{X}^{IFS}) = \sum_{i=1}^{c}\sum_{j=1}^{N}(u_{ij})^m d^2(\mathbf{x}_j^{IFS}, \mathbf{v}_i^{IFS}) \\ \text{subject to} \sum_{i=1}^{c} u_{ij} = 1, \quad 1 \le j \le N \end{cases} \tag{26}$$

where $\boldsymbol{X}^{IFS} = (\boldsymbol{x}_1^{IFS}, x_2^{IFS}, \ldots, \boldsymbol{x}_N^{IFS})$ are N intuitionistic fuzzy data and each $\mathbf{x}_j^{IFS}$ is represented in terms of IFS as $\mathbf{x}_j^{IFS} = (\mu(x_j), \nu(x_j), \pi(x_j))$, $m(1 < m < \infty)$ is the fuzzifier constant, $c(1 < c < N)$ is the number of clusters, $\mathbf{V}^{IFS} = (\mathbf{v}_1^{IFS}, \mathbf{v}_2^{IFS}, \ldots, \mathbf{v}_c^{IFS})$ are centroids of cluster and each v_i^{IFS} is represented in terms of IFS as $\mathbf{v}_i^{IFS} = (\mu(v_i), \nu(v_i), \pi(v_i))$, $u_{ij}(0 \le u_{ij} \le 1)$ denotes the membership degree and $\mathbf{U} = (u_{ij})_{c\times N}$ is membership matrix. The membership matrix U also satisfies the condition $0 < \sum_{j=1}^{N} u_{ij} < N, \quad \forall i$. The term $d^2(\mathbf{x}_j^{IFS}, \mathbf{v}_i^{IFS})$ is the Euclidean intuitionistic fuzzy distance between the data $\mathbf{x}_j^{IFS}$ and centroids $\mathbf{v}_i^{IFS}$, which is defined [33] as:

$$d^2(\mathbf{x}_j^{IFS}, \mathbf{v}_i^{IFS}) = ((\mu(x_j) - \mu(v_i))^2 + (\nu(x_j) - \nu(v_i))^2 + (\pi(x_j) - \pi(v_i))^2) \tag{27}$$

The non-linear optimization problem (26) of the IFCM algorithm can be solved using Lagrangian multiplier method and its membership and centroids $\mathbf{v}_i^{IFS} = (\mu(v_i), \nu(v_i), \pi(v_i))$ are given [23] as:

$$u_{ij} = \frac{1}{\sum_{r=1}^{c}\left(\frac{d^2(\mathbf{x}_j^{IFS}, \mathbf{v}_i^{IFS})}{d^2(\mathbf{x}_j^{IFS}, \mathbf{v}_r^{IFS})}\right)^{\frac{1}{m-1}}}, \quad 1 \le i \le c,\ 1 \le j \le N \tag{28}$$

$$\mu(v_i) = \frac{\sum_{j=1}^{N} u_{ij}^m \mu(x_j)}{\sum_{j=1}^{N} u_{ij}^m}, \quad 1 \le i \le c \tag{29}$$

$$\nu(v_i) = \frac{\sum_{j=1}^{N} u_{ij}^m \nu(x_j)}{\sum_{j=1}^{N} u_{ij}^m}, \quad 1 \le i \le c \tag{30}$$

$$\pi(v_i) = \frac{\sum_{j=1}^{N} u_{ij}^m \pi(x_j)}{\sum_{j=1}^{N} u_{ij}^m}, \quad 1 \le i \le c \tag{31}$$

The outline of the IFCM algorithm is given [23] as follows:

Algorithm 6. Intuitionistic fuzzy c-means (IFCM) algorithm

Step 1: Set the number of clusters c, fuzzifier constant m and stopping criterion ε
Step 2: Calculates $\mathbf{x}_j^{IFS} = (\mu(x_j), \nu(x_j), \pi(x_j)), for\, j = 1, 2, \ldots, N$ using Eq. (8), Eq. (4) and Eq. (2)
Step 3: Initialize the membership degree $\mathbf{U}^{(0)}$ with setting the loop counter $a = 0$
Step 4: Compute the centroids $(\mathbf{v}_i^{IFS})^{(a)} = ((\mu(v_i))^{(a)}, (\nu(v_i))^{(a)}, (\pi(v_i))^{(a)})$ using Eqs. (29–31) and $d^2(\mathbf{x}_j^{IFS}, (\mathbf{v}_i^{IFS})^{(a)})$ using Eq. (27)
Step 5: Compute the membership degrees $\mathbf{U}^{(a+1)}$ using Eq. (28)
Step 6: Stop if $\max \left\|\mathbf{U}^{(a+1)} - \mathbf{U}^{(a)}\right\| < \varepsilon$, otherwise set counter $a = a + 1$ and go to step 4

4. Proposed algorithm

The IFCM algorithm has two drawbacks: (i) the objective function (Eq. (26)) of the IFCM algorithm does not incorporates any local spatial information as it deals each pixel as a separate point. Generally, noise in the image occurs during image acquisition process, which may change the intensity value of pixel. So, the noisy pixels are always wrongly classified in an image because it shows the abnormal behavior in that neighborhood. (ii) The membership degree of the IFCM (Eq. (28)) is a function of distance between gray-level value and cluster center. The high membership degree is assigned to that pixels which are close to the centroids and low membership degree is assigned to those pixels which are far from the centroids. Hence, the membership degree is sensitive in the presence of noise [2].

To some extent, FGFCM, EnFCM, FCM_S1 and FCM_S2 handle the noise during clustering and yield effective segmentation results. However, these algorithms employ parameters α (or λ_g and λ_s) and the performance of segmentation depends on the choice of parameters, whose tuning is computationally intensive. Also, these algorithms are unable to handle the uncertainty. The improved fuzzy c-means (ImFCM) algorithm employs two parameters β and ψ. These two parameters are learned using artificial neural network model [2] and require huge computation time. The FLICM algorithm does not require the parameter tuning α (or λ_g and λ_s) and also improved the segmentation performance but it is unable to handle the uncertainty.

To overcome the problems of these research works, we have proposed an improved intuitionistic fuzzy c-means (IIFCM) algorithm for robust and fast segmentation, which is described in following two subsections.

4.1. Novel intuitionistic fuzzy factor

In order to incorporates both local gray-level and spatial information, a novel intuitionistic fuzzy factor is required in the objective function of IFCM algorithm. The intuitionistic fuzzy factor has the following characteristics:

- It does not requires any parameter tuning;
- It incorporates both local gray-level and spatial information in an intuitionistic fuzzy manner to maintain the noise insensitiveness and robustness;
- It considers similarity of pixels in a specified window during clustering process.

Mathematically, the novel intuitionistic fuzzy factor H_{ij} is written as

$$H_{ij} = \frac{1}{N_R}\sum_{k\in N_j}\frac{1}{d_{jk}+1}[(1-u_{ik})^m + (s_{ik})^m] \quad 1 \le i \le c,\ 1 \le j \le N \tag{32}$$

where kth pixel is a neighboring pixel around the centered jth pixel, N_j represents the number of neighboring pixels around the centered pixel x_j, N_R denotes the cardinality of N_j, u_{ik} denotes the membership degree of kth pixel to the ith cluster center, $m(1 < m < \infty)$ is the fuzzifier constant, and s_{ik} is the similarity measure between kth pixel to the ith cluster which is defined in Eq. (6). The term $d_{jk} = \sqrt{(p_j - p_k)^2 + (q_j - q_k)^2}$ is the spatial Euclidean distant between spatial coordinates (p_j, q_j) and (p_k, q_k) corresponding to the jth and kth pixels respectively.

The intuitionistic fuzzy factor H_{ij} is determined by sliding a fixed size window across every pixel in the image. This intuitionistic fuzzy factor includes the local gray-level information by considering the similarity measures and membership degree, whose objective is to maximize the membership degree and similarity measure into a specified local window. In addition to quantitative measures, similarity measure also considers the qualitative information by utilizing the advantage of intuitionistic fuzzy sets theory. On the other hand, the local spatial information is included

by introducing the distance d_{jk}. The intuitionistic fuzzy factor H_{ij} is completely free of any parameter (α, λ_g, λ_s, etc.) setting, which is required to control the balance between preserving image details and robustness to noise, and this balance is achieved by intuitionistic fuzzy factor. The role of the novel intuitionistic fuzzy factor H_{ij} during the image segmentation will be illustrated in the following section.

4.2. Formulation of the improved intuitionistic fuzzy c-means (IIFCM) algorithm

In this section, we formulate a novel algorithm for image segmentation, named the improved intuitionistic fuzzy c-means (IIFCM) by combining the advantage of IFCM, FLICM and intuitionistic fuzzy sets theory, and introducing the intuitionistic fuzzy factor H_{ij}. With the inclusion of the intuitionistic fuzzy factor H_{ij}, the IIFCM algorithm incorporates both local gray-level and spatial information. It also utilizes the qualitative information, which is obtained via intuitionistic membership μ_p and non-membership degree ν_p for each data point x_p. The proposed algorithm aims to overcome the problem of noise by incorporating the local spatial information and to handle the uncertainty between the complex boundaries in the medical images by utilizing the advantage of intuitionistic fuzzy sets theory. The non-linear optimization problem of the IIFCM algorithm is defined as:

$$\begin{cases} \min A_m(\mathbf{U}, \mathbf{V}^{IFS} : \mathbf{X}^{IFS}) = \sum_{i=1}^{c}\sum_{j=1}^{N}(u_{ij})^m d^2(\mathbf{x}_j^{IFS}, \mathbf{v}_i^{IFS})H_{ij} \\ \text{subject to} \sum_{i=1}^{c} u_{ij} = 1, \quad 1 \le j \le N \end{cases} \tag{33}$$

where $\mathbf{X}^{IFS} = (\mathbf{x}_1^{IFS}, \mathbf{x}_2^{IFS}, \ldots, \mathbf{x}_N^{IFS})$ are N intuitionistic fuzzy data, $m(1<m<\infty)$ is the fuzzifier constant, $c(1<c<N)$ is the number of clusters, $\mathbf{V}^{IFS} = (\mathbf{v}_1^{IFS}, \mathbf{v}_2^{IFS}, \ldots, \mathbf{v}_c^{IFS})$ are centroids of cluster and each $\mathbf{v}_i^{IFS}$ is represented in terms of IFS as $\mathbf{v}_i^{IFS} = (\mu(v_i), \nu(v_i), \pi(v_i))$, $u_{ij}(0 \le u_{ij} \le 1)$ denote the membership degree, $\mathbf{U} = (u_{ij})_{c\times N}$ is the membership matrix, H_{ij} is intuitionistic fuzzy factor which is defined in Eq. (32). The term $d^2(\mathbf{x}_j^{IFS}, \mathbf{v}_i^{IFS})$ is the Euclidean intuitionistic fuzzy distance between the data $\mathbf{x}_j^{IFS}$ and centroids $\mathbf{v}_i^{IFS}$ as defined in Eq. (27). We have used Lagrangian multiplier method to solve the optimization problem (33). Let the Lagrangian function of the IIFCM algorithm is written as:

$$A_m^*(\mathbf{V}, \mathbf{V}^{IFS}; \mathbf{X}^{IFS}, \mathbf{k}) = \sum_{i=1}^{c}\sum_{j=1}^{N}(u_{ij})^m d^2(\mathbf{x}_j^{IFS}, \mathbf{v}_i^{IFS})H_{ij} - \sum_{j=1}^{N} k_j \left(\sum_{i=1}^{c} u_{ij} - 1\right) \tag{34}$$

where k_j denote the Lagrangian multiplier constants. Calculating the partial derivatives of A_m^* with respect to u_{ij} and k_j and equating them zero, we have

$$\underset{\substack{1\le j\le N\\ 1\le i\le c}}{\forall} \frac{\partial A_m^*}{\partial u_{ij}} = 0 \text{ and } \underset{1\le j\le N}{\forall} \frac{\partial A_m^*}{\partial k_j} = 0 \tag{35}$$

After simplifying Eq. (35), we get

$$u_{ij} = \frac{1}{\sum_{r=1}^{c}\left(\frac{d^2(\mathbf{x}_j^{IFS}, \mathbf{v}_i^{IFS})H_{ij}}{d^2(\mathbf{x}_j^{IFS}, \mathbf{v}_r^{IFS})H_{rj}}\right)^{\frac{1}{m-1}}}, \quad 1 \le i \le c, 1 \le j \le N \tag{36}$$

Similarly, calculate the partial derivatives of A_m^* with respect to $\mu(v_i)$, $\nu(v_i)$ and $\pi(v_i)$, and equate them zero, we have

$$\underset{\substack{1\le j\le N\\ 1\le i\le c}}{\forall} \frac{\partial A_m^*}{\partial \mu(v_i)} = \frac{\partial A_m^*}{\partial \nu(v_i)} = \frac{\partial A_m^*}{\partial \pi(v_i)} = 0 \tag{37}$$

Now simplifying Eq. (37), we obtained

$$\mu(v_i) = \frac{\sum_{j=1}^{N} u_{ij}^m \mu(x_j)}{\sum_{j=1}^{N} u_{ij}^m}, \quad 1 \le i \le c \tag{38}$$

$$\nu(v_i) = \frac{\sum_{j=1}^{N} u_{ij}^m \nu(x_j)}{\sum_{j=1}^{N} u_{ij}^m}, \quad 1 \le i \le c \tag{39}$$

$$\pi(v_i) = \frac{\sum_{j=1}^{N} u_{ij}^m \pi(x_j)}{\sum_{j=1}^{N} u_{ij}^m}, \quad 1 \le i \le c \tag{40}$$

From Eqs. (38)–(40), the centroids $\mathbf{V}^{IFS} = (\mathbf{v}_1^{IFS}, \mathbf{v}_2^{IFS}, \ldots, \mathbf{v}_c^{IFS})$ of the IIFCM are defined as:

$$\mathbf{v}_i^{IFS} = (\mu(v_i), \nu(v_i), \pi(v_i)) \tag{41}$$

The IIFCM algorithm is summarized as:

Algorithm 7. Improved intuitionistic fuzzy c-means (IIFCM) algorithm

Step 1: Set the number of clusters c, fuzzifier constant m and stopping criterion ε
Step 2: Calculates $\mathbf{x}_j^{IFS} = (\mu(x_j), \nu(x_j), \pi(x_j))$, *for* $j = 1, 2, \ldots, N$ using Eq. (8), Eq. (4) and Eq. (2)
Step 3: Initialize the membership degree $\mathbf{U}^{(0)}$ with setting the loop counter $a = 0$
Step 4: Compute the centroids $(\mathbf{v}_i^{IFS})^{(a)} = ((\mu(v_i))^{(a)}, (\nu(v_i))^{(a)}, (\pi(v_i))^{(a)})$ using Eqs. (38–40) and $d^2(\mathbf{x}_j^{IFS}, (\mathbf{v}_i^{IFS})^{(a)})$ using Eq. (27)
Step 5: Compute the similarity measure s_{ik} using Eq. (6)
Step 6: Compute the intuitionistic fuzzy factor $H_{ij}^{(a)}$ using Eq. (32)
Step 7: Compute the membership degrees $\mathbf{U}^{(a+1)}$ using Eq. (36)
Step 8: Stop if max $\left\|\mathbf{U}^{(a+1)} - \mathbf{U}^{(a)}\right\| < \varepsilon$, otherwise set counter $a = a + 1$ and go to step 4

The summary of parameters and procedures for above segmentation algorithms: FCM_S1, FCM_S2, EnFCM, FGFCM, FLICM, IFCM and IIFCM are given in Table 1.

5. Experimental results and discussion

To demonstrate the efficacy of the proposed IIFCM algorithm, experiment is carried out on synthetic square image and two publically available MRI brain images. The segmentation performance of the IIFCM method is compared with seven existing methods: IFCM, FLICM, EnFCM, ImFCM, FGFCM, FCM_S1 and FCM_S2. These algorithms are implemented in Matlab.

The segmentation results are compared quantitatively in the term of similarity index (ρ), false negative ratio (r_{fn}) and false positive ratio (r_{fp}). These performance measures are calculated as [34]:

$$\rho = \frac{2|X_i \cap Y_i|}{|X_i| + |Y_i|} \tag{42}$$

$$r_{fn} = \frac{|X_i| - |X_i \cap Y_i|}{|X_i|} \tag{43}$$

$$r_{fp} = \frac{|Y_i| - |X_i \cap Y_i|}{|X_i|} \tag{44}$$

Table 1
Summary of parameter and procedures for different segmentation algorithms.

Algorithms	Parameters	Algorithm procedures
FCM_S1	m, c, α	Compute the mean filtered image Initialize the membership degree U Update the centroids v_i using Eq. (14) Update the membership degrees U using Eq. (13) Check the convergence
FCM_S1	m, c, α	Compute the median filtered image Initialize the membership degree **U** Update the centroids v_i using Eq. (14) Update the membership degrees **U** using Eq. (13) Check the convergence
EnFCM	m, c, α	Compute the new image ξ using Eq. (15) Initialize the membership degree **U** Update the centroids v_i using Eq. (18) Update the membership degrees **U** using Eq. (17) Check the convergence
FGFCM	$m, c, \lambda_s, \lambda_g$	Compute the similarity measure S_{ij} using Eq. (19) Compute the new sum image ξ using Eq. (21) Initialize the membership degree **U** Update the centroids v_i using Eq. (18) Update the membership degrees **U** using Eq. (17) Check the convergence
FLICM	m, c	Initialize the membership degree **U** Update the centroids v_i using Eq. (25) Update the fuzzy factor G_{ij} using Eq. (23) Update the membership degrees **U** using Eq. (24) Check the convergence
IFCM	m, c, λ	Calculates $\boldsymbol{x}_j^{IFS}$ using Eq. (8), Eq. (4) and Eq. (2) Initialize the membership degree **U** Update the centroids $\boldsymbol{v}_i^{IFS}$ using Eqs. (29–31) Update the membership degrees **U** using Eq. (28) Check the convergence
IIFCM	m, c, λ	Calculates $\boldsymbol{x}_j^{IFS}$ using Eq. (8), Eq. (4) and Eq. (2) Initialize the membership degree **U** Update the centroids $\boldsymbol{v}_i^{IFS}$ using Eqs. (38–40) Update the similarity measure s_{ik} using Eq. (6) Update the intuitionistic fuzzy factor $H_{ij}^{(a)}$ using Eq. (32) Update the membership degrees **U** using Eq. (36) Check the convergence

where X_i denote the pixels belonging to the manual segmented image, Y_i denote the pixels belonging to the experimental segmented image and $|X_i|$ denotes the cardinality of X_i.

5.1. Synthetic square image

In this section, we demonstrate the performance of proposed IIFCM algorithms on a synthetic generated square image of size 140×140 pixels. The intensity values of synthetic square image (Fig. 1(a)) are 80, 130, 190 and 250 corresponding to four different classes, namely class_1 (intensity value 80), class_2 (intensity value 130), class_3 (intensity value 190) and class_4 (intensity value 250). To check the robustness of method in presence of noise, we have introduced salt and pepper 1% noise in the original square image (Fig. 1(a)), which is shown in Fig. 1(b). Further, for quantitatively comparison, we have generated the ground truth square image corresponding to four classes, which is shown in Fig. 1(c). In the experiment setup for synthetic square image, we set the value of parameters $\lambda_s(=3)$ and window size 3×3 ($N_R = 8$) [19]. The number of clusters c is set to 4 corresponding to four classes. Initially, we carried out experiment for different values of λ, but we observed that segmentation result for synthetic square image is better for $\lambda(=1.5)$ in IIFCM and IFCM algorithms. The segmented image of corrupted square image (Fig. 1(b)) by IIFCM and IFCM algorithms are depicted in Fig. 1(d) and (e) respectively. Fig. 1(f)–(j) shows the segmented square image by FLICM, EnFCM, FGFCM, FCM_S1 and FCM_S2 algorithms respectively. The value of parameter α in EnFCM, FCM_S1, FCM_S2 is chosen 0.2 after searching optimal value in the interval [0.2, 8] with increment 0.2. In the FGFCM algorithms, the value of parameter λ_g is set to equal to 0.6 after searching the optimal value in the interval [0.5, 6] with increment 0.5. The segmented square image by ImFCM is shown in Fig. 1(k), where the value of learning rate is set to equal to 0.2. Visually, Fig. 1(h) shows that the FGFCM removes most of salt and pepper 1% noise, but its similarity value is less than other algorithms. The IIFCM (Fig. 1(d)) removes salt and pepper 1% noise and achieves the best performance, which is shown in Table 2.

Furthermore, we have applied above eight algorithms on the square image which is corrupted by salt and pepper 5% noise, Poisson noise and Gaussian 1% noise. The comparison in the term of similarity index (ρ), false negative ratio (r_{fn}) and false positive ratio (r_{fp}) of all the eight algorithms are shown in Tables 2, 3 and 4 respectively. It can be noted from Table 2 that the similarity index (ρ) of the proposed IIFCM algorithm is more than existing algorithms except the Poisson noise (class_3) and Gaussian 1% noise. The segmentation results of the IIFCM algorithm is the second best for the Gaussian 1% noise (class_1 and class_2). It also observed from Table 2, as the value of salt and pepper increases from 1% to 5%, the value of similarity index (ρ) decreases. Also, it can be noted from Tables 3 and 4 that the value of r_{fp} and r_{fn} are minimum in most of the cases for the proposed IIFCM algorithm.

5.2. The MRI brain images

In this section, the efficacy of the proposed method IIFCM is checked on two publically available brain databases: (i) simulated brain data [35] and (ii) real MRI brain data [36]. The non-brain tissues are removed prior to applying the segmentation algorithms with Brain Extraction Tool (BET) [37]. In the experimental setup for all brain images (simulated and real), we set the value of parameter $\lambda_s(=3)$, window size 3×3 ($N_R = 8$) [19]. We fixed the fuzzifier constant $m = 2$ and number of cluster $c = 4$ corresponding to GM, WM, CSF and background. The experiment is carried out for different values of λ, but we observed that segmentation result is better for $\lambda(=1.5)$ in IIFCM and IFCM algorithms. Also, we set $\alpha(=0.2)$ in EnFCM, FCM_S1 and FCM_S2 algorithms after searching optimal value in the interval [0.2, 8] with increment 0.2. The value of parameter λ_g is set to equal to 0.6 in the FGFCM after searching the optimal value in the interval [0.5, 6] with increment 0.5. In the ImFCM algorithm, the value of learning rate is chosen 0.2.

5.2.1. Simulated brain images

The simulated brain images are acquired from Brain Web [35], where ground truth images are also publically available. We have evaluated segmentation performance on 2D axial view of T1-weighted simulated brain images of slice thickness 1 mm with different intensity non-uniformity (INU = 0 and INU = 20) and noise level (0%, 1% and 3%). The brain images are segmented into four classes: cerebrospinal fluid (CSF), white matter (WM), gray matter (GM) and background. In the quantitative measure the background part is not considered.

The simulated brain image (Fig. 2(b)) of size 217×181, is a slice of 3D brain data with 1% noise (INU = 0) and its segmented image consisting of CSF, GM, and WM are visually depicted in Fig. 2(c). These manual segmented images are used to validate the proposed segmentation method. Considering the optimal parameters as mentioned above for brain images, we have applied eight algorithms on original simulated brain image (Fig. 2(b)) and evaluated their performance in terms of ρ, r_{fp} and r_{fn} for GM and WM, which are shown in Tables 5 and 6 respectively. Fig. 2(d)–(k) visually show the segmented image of the original brain image (Fig. 2(b)) by IIFCM, IFCM, FLICM, EnFCM, FGFCM, FCM_S1, FCM_S2 and ImFCM algorithms respectively. From Tables 5 and 6, it can be noted that the similarity index (ρ) of IIFCM on the image (Fig. 2(b)) is more than

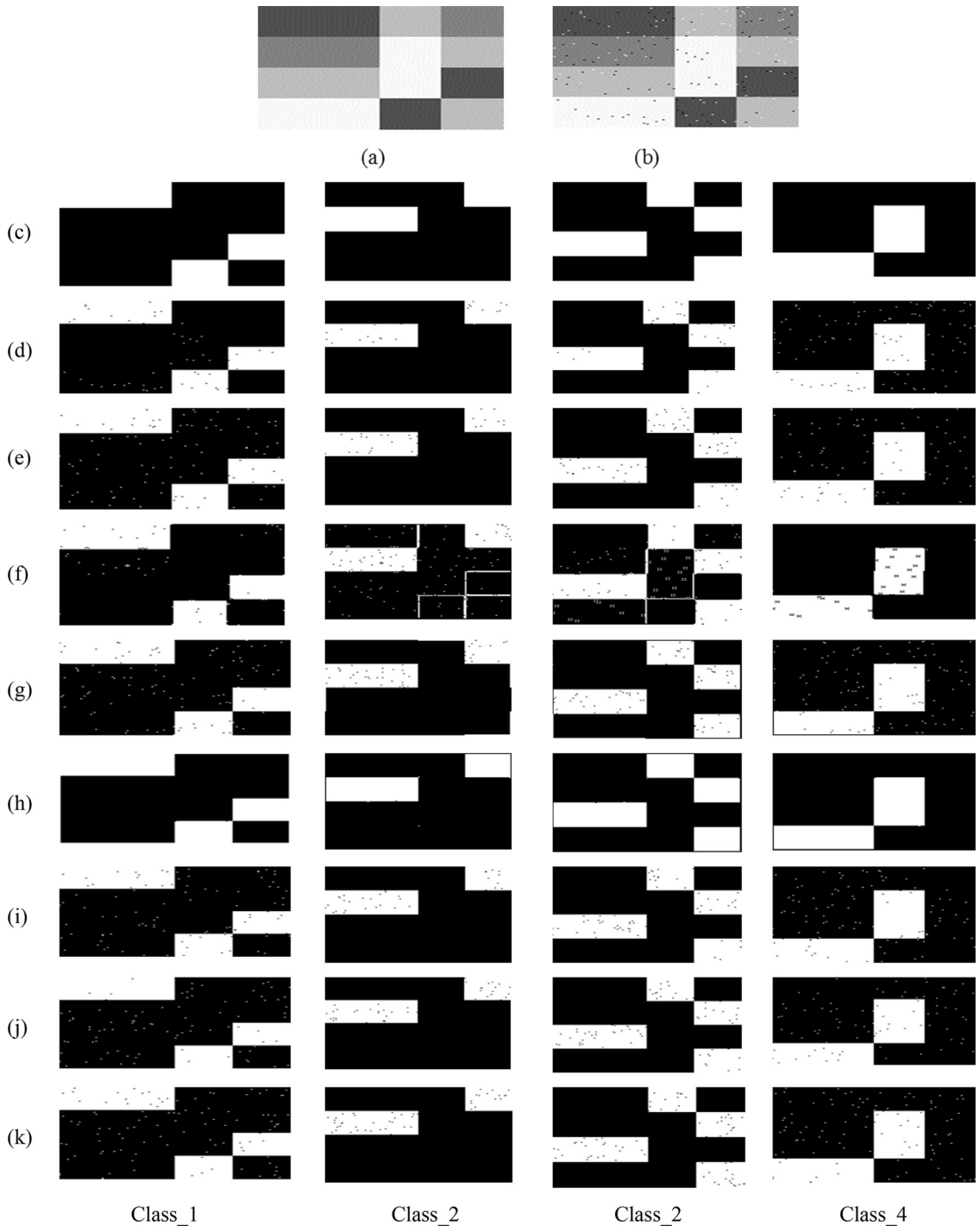

Fig. 1. Original and segmented square image by different algorithm: (a) square image (b) square image corrupted by salt and pepper 1% noise, (c) ground truth square image, (d) IIFCM algorithm, (e) IFCM algorithm, (f) FLICM algorithm, (g) EnFCM algorithm, (h) FGFCM algorithm, (i) FCM_S1 algorithm, (j) FCM_S2 algorithm, (k) ImFCM algorithm.

existing algorithms for GM and WM. Also, the false negative ratio (r_{fn}) and false positive ratio (r_{fp}) of the proposed IIFCM algorithm is minimum.

Further, we have evaluated above eight algorithms on other simulated brain images with different intensity non-uniformity (INU = 0 and INU = 20) and noise levels (0%, 1% and 3%), and computed their performance in terms of ρ, r_{fp} and r_{fn} for GM and WM, which are shown in Tables 5 and 6 respectively. From Tables 5 and 6, it can be observed that the similarity index (ρ) of the proposed method IIFCM is more than other algorithms for GM and WM. And, the false negative ratio (r_{fn}) and false positive ratio (r_{fp}) are minimum for most of the images for the proposed IIFCM algorithm.

5.2.2. Real brain images

In this section, we used real MRI brain images from the Internet Brain Segmentation Repository (IBSR), where manually segmented images are also available for validation of new segmentation methods. We have tested IIFCM, IFCM, ImFCM, FGFCM, FLICM, EnFCM, FCM_S1 and FCM_S2 algorithms on 2D axial slices of T1-weighted real brain images.

Table 2
Comparison of different segmentation algorithms in terms of similarity index (ρ) on synthetic square image with different noise.

Class	Noise	IIFCM	IFCM	FLICM	EnFCM	FGFCM	FCM_S1	FCM_S2	ImFCM
Class_1	Salt and pepper 1%	0.9948	0.9902	0.9710	0.9894	0.9623	0.9900	0.9908	0.9891
	Salt and pepper 5%	0.9722	0.9522	0.9073	0.9499	0.9565	0.9504	0.9565	0.9464
	Poisson	0.9996	0.9875	0.9764	0.9938	0.9621	0.9975	0.9978	0.9928
	Gaussian 1%	0.9696	0.8485	0.9717	0.9581	0.9556	0.8539	0.8498	0.8163
Class_2	Salt and pepper 1%	0.9970	0.9960	0.9337	0.9706	0.9850	0.9955	0.9943	0.9936
	Salt and pepper 5%	0.9870	0.9779	0.8348	0.9545	0.9804	0.9762	0.9749	0.9729
	Poisson	0.9938	0.9694	0.9543	0.9726	0.9844	0.9924	0.9919	0.9774
	Gaussian 1%	0.9364	0.7829	0.9485	0.9113	0.9712	0.7308	0.7338	0.6665
Class_3	Salt and pepper 1%	0.9975	0.9951	0.9630	0.9714	0.9852	0.9952	0.9945	0.9943
	Salt and pepper 5%	0.9853	0.9764	0.9149	0.9516	0.9783	0.9733	0.9779	0.9712
	Poisson	0.9858	0.9729	0.9784	0.9718	0.9844	0.9898	0.9834	0.9742
	Gaussian 1%	0.9504	0.9118	0.9767	0.9521	0.9802	0.8282	0.8376	0.7772
Class_4	Salt and pepper 1%	0.9921	0.9918	0.9732	0.9788	0.9891	0.9896	0.9913	0.9895
	Salt and pepper 5%	0.9553	0.9546	0.9200	0.9416	0.9531	0.9523	0.9540	0.9473
	Poisson	0.9865	0.9774	0.9852	0.9793	0.9823	0.9804	0.9803	0.9778
	Gaussian 1%	0.9600	0.9421	0.9827	0.9665	0.9860	0.8855	0.8945	0.8581

Table 3
Comparison of different segmentation algorithms in terms of false negative ratio (r_{fn}) on synthetic square image with different noise.

Class	Noise	IIFCM	IFCM	FLICM	EnFCM	FGFCM	FCM_S1	FCM_S2	ImFCM
Class_1	Salt and pepper 1%	0.0050	0.0051	0.0510	0.0055	0.0054	0.0067	0.0062	0.0053
	Salt and pepper 5%	0.0035	0.0273	0.1463	0.0253	0.0051	0.0241	0.0245	0.0278
	Poisson	0.0006	0.0231	0.0459	0.0012	0.0006	0.0018	0.0008	0.0029
	Gaussian 1%	0.0502	0.2571	0.0508	0.0329	0.0647	0.2092	0.2271	0.2624
Class_2	Salt and pepper 1%	0.0057	0.0079	0.0212	0.0125	0.0286	0.0090	0.0114	0.0128
	Salt and pepper 5%	0.0256	0.0433	0.0661	0.0463	0.0337	0.0465	0.0484	0.0528
	Poisson	0.0005	0.0082	0.0087	0.0163	0.0291	0.0057	0.0052	0.0180
	Gaussian 1%	0.0299	0.1246	0.0180	0.0854	0.0446	0.2152	0.2014	0.2536
Class_3	Salt and pepper 1%	0.0051	0.0098	0.0278	0.0395	0.0289	0.0095	0.0109	0.0114
	Salt and pepper 5%	0.0291	0.0462	0.0557	0.0754	0.0374	0.0519	0.0433	0.0560
	Poisson	0.0112	0.0318	0.0163	0.0318	0.0296	0.0124	0.0175	0.0323
	Gaussian 1%	0.0717	0.0922	0.0165	0.0696	0.0358	0.2103	0.1966	0.2575
Class_4	Salt and pepper 1%	0.0037	0.0039	0.0516	0.0253	0.0214	0.0045	0.0047	0.0043
	Salt and pepper 5%	0.0215	0.0229	0.1445	0.0490	0.0255	0.0257	0.0220	0.0267
	Poisson	0.0190	0.0231	0.0276	0.0294	0.0222	0.0090	0.0092	0.0218
	Gaussian 1%	0.0180	0.0188	0.0296	0.0178	0.0229	0.0467	0.0382	0.0884

The skull stripping real brain image (Fig. 3(b)) of size 64×146 pixels, is a slice of 3D real brain data (case 111_2) and its manually segmented image consisting of CSF, GM, and WM are visually depicted in Fig. 3(c). We have considered optimal parameters discussed above (Section 5.2) of each algorithm for segmentation. Fig. 3(d)–(k) visually shows the segmented images of the original image (Fig. 3(b)) by IIFCM, IFCM, FLICM, EnFCM, FGFCM, FCM_S1, FCM_S2 and ImFCM algorithms respectively. Similarly, we applied eight algorithms on 30 different real brain images and computed their performance measure for GM. The average performance in

Table 4
Comparison of different segmentation algorithms in terms of false positive ratio (r_{fp}) on synthetic square image with different noise.

Class	Noise	IIFCM	IFCM	FLICM	EnFCM	FGFCM	FCM_S1	FCM_S2	ImFCM
Class_1	Salt and pepper 1%	0.0051	0.0145	0.0057	0.0157	0.0780	0.0133	0.0163	0.0165
	Salt and pepper 5%	0.0224	0.0704	0.0282	0.0776	0.0853	0.0778	0.0643	0.0824
	Poisson	0.0002	0.0016	0.0002	0.0112	0.0782	0.0033	0.0037	0.0116
	Gaussian 1%	0.0030	0.0082	0.0049	0.0518	0.0878	0.0614	0.0461	0.0696
Class_2	Salt and pepper 1%	0.0000	0.0000	0.1178	0.0473	0.0011	0.0000	0.0000	0.0000
	Salt and pepper 5%	0.0000	0.0000	0.3034	0.0446	0.0049	0.0000	0.0005	0.0000
	Poisson	0.0020	0.0544	0.0863	0.0392	0.0016	0.0095	0.0112	0.0275
	Gaussian 1%	0.1018	0.3608	0.0887	0.0925	0.0120	0.3630	0.3780	0.4933
Class_3	Salt and pepper 1%	0.0000	0.0000	0.0469	0.0171	0.0003	0.0000	0.0000	0.0000
	Salt and pepper 5%	0.0000	0.0000	0.1200	0.0186	0.0052	0.0000	0.0000	0.0000
	Poisson	0.0122	0.0220	0.0271	0.0243	0.0011	0.0080	0.0075	0.0189
	Gaussian 1%	0.0251	0.0833	0.0305	0.0240	0.0033	0.1174	0.1149	0.1682
Class_4	Salt and pepper 1%	0.0005	0.0127	0.0006	0.0169	0.0002	0.0165	0.0129	0.0169
	Salt and pepper 5%	0.0054	0.0700	0.0063	0.0690	0.0071	0.0718	0.0722	0.0816
	Poisson	0.0118	0.0220	0.0016	0.0116	0.0008	0.0102	0.0143	0.0227
	Gaussian 1%	0.0639	0.1018	0.0045	0.0504	0.0049	0.1998	0.1888	0.2131

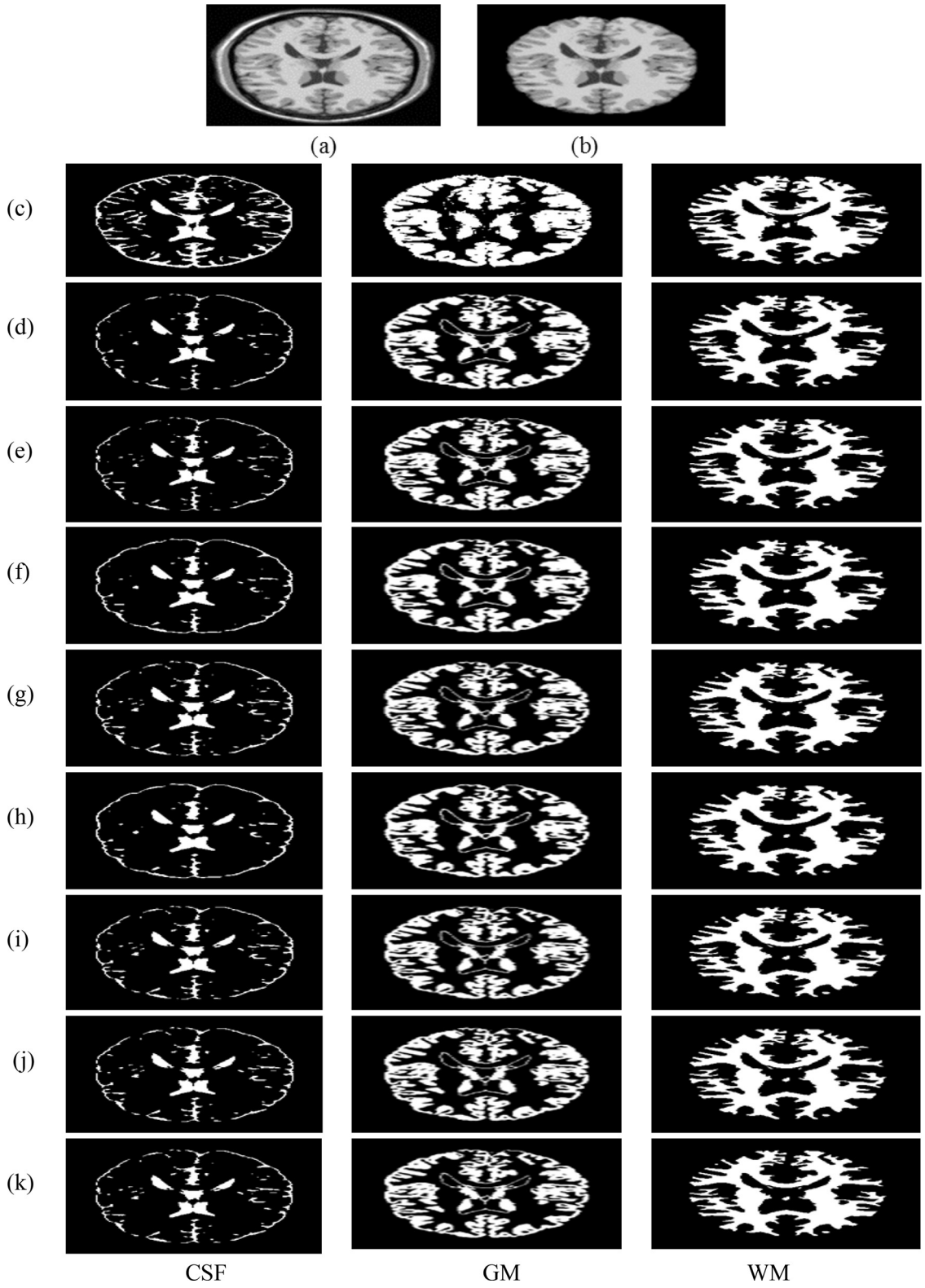

Fig. 2. Original and segmented simulated brain image by different algorithms: (a) axial view of original simulated T1-weighted brain image with INU = 0 and 1% noise, (b) skull stripping simulated brain image, (c) manual segmented CSF, GM and WM images, (d) IIFCM algorithm, (e) IFCM algorithm, (f) FLICM algorithm, (g) EnFCM algorithm, (h) FGFCM algorithm, (i) FCM_S1 algorithm, (j) FCM_S2 algorithm, (k) ImFCM algorithm.

terms of ρ, r_{fp} and r_{fn} is shown in Table 7. From Table 7, it can be observed that the proposed IIFCM method achieves the best performance.

Further, to study the statistical significance of the performance of various segmentation algorithms, we have used the Friedman's statistical test [38] which has been used in the recent research work [39]. It is two-way analysis of variance of ranks in which the null hypothesis (H_0) is defines the performance of all the segmentation algorithms are equal in terms of a given measure (ρ, r_{fn}, r_{fp}) against the alternative hypothesis (H_1) that is the performance of

Table 5
Comparative performance (ρ, r_{fp}, r_{fn}) of different segmentation algorithms on simulated brain images with different INU and noise levels for GM.

INU	Performance measure	Noise	IIFCM	IFCM	FLICM	EnFCM	FGFCM	FCM_S1	FCM_S2	ImFCM
INU = 0	ρ	0%	0.8284	0.8252	0.8266	0.8222	0.8170	0.8214	0.8256	0.8244
		1%	0.8256	0.8223	0.8253	0.8195	0.8166	0.8197	0.8235	0.8241
		3%	0.8255	0.8245	0.8251	0.8192	0.8137	0.8187	0.8205	0.8182
	r_{fp}	0%	0.0214	0.0216	0.0274	0.0222	0.0255	0.0221	0.0217	0.0218
		1%	0.0216	0.0218	0.0273	0.0223	0.0255	0.0224	0.0219	0.0220
		3%	0.0212	0.0212	0.0275	0.0215	0.0258	0.0215	0.0205	0.0204
	r_{fn}	0%	0.2761	0.2825	0.2763	0.2864	0.2918	0.2877	0.2817	0.2834
		1%	0.2816	0.2866	0.2773	0.2903	0.2924	0.2899	0.2846	0.2837
		3%	0.2822	0.2837	0.2785	0.2914	0.2964	0.2920	0.2902	0.2936
INU = 20	ρ	0%	0.8330	0.8313	0.8326	0.8301	0.8256	0.8294	0.8316	0.8318
		1%	0.8335	0.8316	0.8321	0.8297	0.8264	0.8284	0.8292	0.8271
		3%	0.8342	0.8332	0.8339	0.8251	0.8212	0.8267	0.8295	0.8275
	r_{fp}	0%	0.0214	0.0217	0.0271	0.0216	0.0257	0.0216	0.0215	0.0216
		1%	0.0212	0.0218	0.0270	0.0219	0.0256	0.0218	0.0216	0.0214
		3%	0.0217	0.0218	0.0280	0.0217	0.0259	0.0220	0.0212	0.0213
	r_{fn}	0%	0.2510	0.2733	0.2585	0.2752	0.2789	0.2762	0.2729	0.2726
		1%	0.2700	0.2727	0.2575	0.2756	0.2778	0.2776	0.2765	0.2797
		3%	0.2606	0.2703	0.2611	0.2825	0.2854	0.2799	0.2764	0.2792

Table 6
Comparative performance (ρ, r_{fp}, r_{fn}) of different segmentation algorithms on simulated brain images with different INU and noise levels for WM.

INU	Performance measure	Noise	IIFCM	IFCM	FLICM	EnFCM	FGFCM	FCM_S1	FCM_S2	ImFCM
INU = 0	ρ	0%	0.9290	0.9286	0.9229	0.9256	0.9264	0.9264	0.9244	0.9236
		1%	0.9300	0.9291	0.9228	0.9263	0.9266	0.9267	0.9250	0.9246
		3%	0.9306	0.9277	0.9230	0.9255	0.9241	0.9263	0.9271	0.9277
	r_{fp}	0%	0.0000	0.0000	0.0001	0.0000	0.0009	0.0000	0.0000	0.0000
		1%	0.0000	0.0000	0.0001	0.0000	0.0011	0.0000	0.0000	0.0000
		3%	0.0004	0.0004	0.0009	0.0004	0.0023	0.0004	0.0004	0.0004
	r_{fn}	0%	0.1325	0.1332	0.1430	0.1385	0.1364	0.1372	0.1406	0.1419
		1%	0.1309	0.1323	0.1433	0.1373	0.1359	0.1366	0.1395	0.1403
		3%	0.1294	0.1346	0.1422	0.1383	0.1391	0.1369	0.1356	0.1346
INU = 20	ρ	0%	0.9246	0.9226	0.9131	0.9201	0.9193	0.9202	0.9197	0.9186
		1%	0.9242	0.9224	0.9137	0.9195	0.9177	0.9211	0.9213	0.9224
		3%	0.9232	0.9196	0.9121	0.9214	0.9190	0.9194	0.9193	0.9196
	r_{fp}	0%	0.0000	0.0000	0.0002	0.0000	0.0018	0.0000	0.0000	0.0000
		1%	0.0000	0.0000	0.0001	0.0000	0.0018	0.0000	0.0000	0.0000
		3%	0.0005	0.0005	0.0012	0.0004	0.0040	0.0003	0.0003	0.0005
	r_{fn}	0%	0.1403	0.1437	0.1598	0.1481	0.1478	0.1478	0.1487	0.1505
		1%	0.1410	0.1441	0.1588	0.1489	0.1505	0.1462	0.1459	0.1441
		3%	0.1422	0.1483	0.1607	0.1453	0.1465	0.1489	0.1491	0.1483

all segmentation algorithms are different. For a given performance measure (M), the H_0 and H_1 are defined as:

$$H_0 : \mu^M_{IIFCM} = \mu^M_{IFCM} = \mu^M_{FLICM} = \mu^M_{EnFCM} = \mu^M_{FGFCM} = \mu^M_{FCM\_S1} = \mu^M_{FCM\_S2} = \mu^M_{ImFCM} \quad (45)$$

and

$$H_1 : \mu^M_{IIFCM} \neq \mu^M_{IFCM} \neq \mu^M_{FLICM} \neq \mu^M_{EnFCM} \neq \mu^M_{FGFCM} \neq \mu^M_{FCM\_S1} \neq \mu^M_{FCM\_S2} \neq \mu^M_{ImFCM} \quad (46)$$

where $M \in \{\rho, r_{fn}, r_{fp}\}$. After ranking different segmentation methods according to each of the three performance measures separately, a comparison of multiple algorithms can be accomplished.

In Friedman test, for each image i, the rank value ranging from 1 (best) to k (worst) is assigned to every algorithm j, which is denoted by $r^j_i (1 \le i \le N,\ 1 \le j \le k)$. The average ranks $R_j = \frac{1}{N}\sum_i r^j_i$ for each algorithm j over all N images are computed. The ranks for all the eight segmentation algorithms computed for each performance measure are shown in Table 8. It can be noted that the best performing IIFCM algorithm has the least rank value for all the three performance measures.

The statistical hypothesis test proposed by Iman and Davenport is used. The statistic F_{ID} is defined by Iman and Davenport [40] as:

$$F_{ID} = \frac{(N-1)\chi^2_F}{N(k-1)-\chi^2_F} \quad (47)$$

Table 7
Average performance measures (ρ, r_{fn}, r_{fp}) for GM on 30 real brain images.

Performance measure	IIFCM	IFCM	FLICM	EnFCM	FGFCM	FCM_S1	FCM_S2	ImFCM
ρ	0.7433	0.7260	0.6533	0.6419	0.6137	0.6246	0.6234	0.6229
r_{fn}	0.1788	0.1862	0.2721	0.2228	0.2565	0.2438	0.2443	0.2459
r_{fp}	0.3076	0.3224	0.3688	0.4134	0.4326	0.4282	0.4295	0.4287

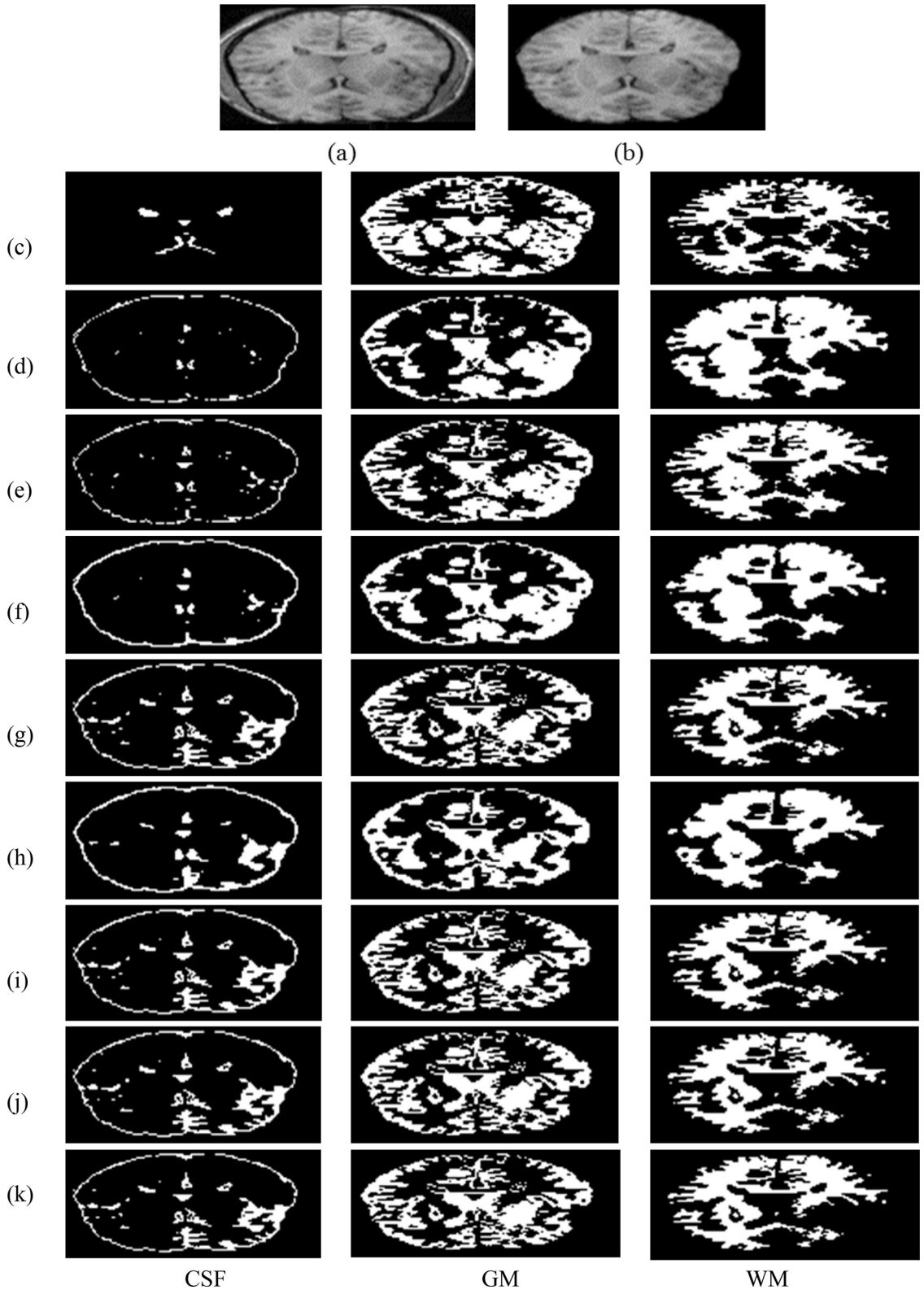

Fig. 3. Original and segmented real brain image by different algorithms: (a) axial view of original T1-weighted real brain image of case 111_2 (b) skull stripping real brain image, (c) manual segmentation image consisting of CSF, GM and WM, (d) IIFCM algorithm, (e) IFCM algorithm, (f) FLICM algorithm, (g) EnFCM algorithm, (h) FGFCM algorithm, (i) FCM_S1 algorithm, (j) FCM_S2 algorithm, (k) ImFCM algorithm.

which is distributed according to F-distribution with $K-1$ and $(k-1)(N-1)$ degrees of freedom, where χ_F^2 is the Friedman's statistic defined as $\frac{12N}{k(k+1)}\left[\sum_j R_j^2 - \frac{k(k+1)^2}{4}\right]$. In our experiments $k=8$ and $N=30$. The p-value computed by Iman and Davenport statistic are 2.03e−27, −2.22e−16 and 4.47e−10 corresponding to performance measures ρ, r_{fn} and r_{fp} respectively, which strongly show the significant differences among the segmentation methods at the significance level of 0.05 and hence rejecting the null hypothesis.

Table 8
Average ranking of the algorithms corresponding to performance measures (ρ, r_{fn}, r_{fp}) for GM using Friedman statistic.

	Performance measure	IIFCM	IFCM	FLICM	EnFCM	FGFCM	FCM_S1	FCM_S2	ImFCM
Rank	ρ	1.43	2.50	4.57	5.50	6.83	5.27	5.18	4.72
	r_{fn}	2.08	2.72	3.23	5.72	6.83	5.12	5.22	5.08
	r_{fp}	2.58	3.07	6.25	4.43	5.57	5.08	4.48	4.53

Table 9
Adjusted p-values corresponding to performance measures (ρ, r_{fn}, r_{fp}) for GM using Friedman test (IIFCM is the control method).

Algorithm	ρ		r_{fn}		r_{fp}	
	Unadjusted p	pHolm	Unadjusted p	pHolm	Unadjusted p	pHolm
FGFCM	1.36e−17	9.55e−17	5.89e−14	4.13e−13	2.39e−06	1.44e−05
EnFCM	1.28e−10	7.66e−10	9.20e−09	5.52e−08	0.003443	0.008191
FCM_S1	1.35e−09	6.76e−09	1.62e−06	6.47e−06	7.72e−05	3.86e−04
FCM_S2	3.04e−09	1.22e−08	7.26e−07	3.63e−06	0.002663	0.008191
ImFCM	2.09e−07	6.26e−07	2.10e−06	6.47e−06	0.002048	0.008191
FLICM	7.26e−07	1.45e−06	0.069017	0.138034	6.73e−09	4.71e−08
IFCM	0.091690	0.091690	0.316639	0.316639	0.444738	0.444738

Table 10
Comparative performance (ρ, r_{fp}, r_{fn}) of different segmentation algorithms on real brain image corrupted by different noise for GM.

Performance measure	Noise	IIFCM	IFCM	FLICM	EnFCM	FGFCM	FCM_S1	FCM_S2	ImFCM
ρ	Salt and pepper 5%	0.7932	0.7856	0.7267	0.6364	0.6746	0.6445	0.6630	0.5871
	Poisson	0.7446	0.7316	0.6956	0.6832	0.6502	0.6719	0.6586	0.6502
	Gaussian 1%	0.6736	0.6715	0.7064	0.6166	0.6359	0.6113	0.6185	0.6124
r_{fp}	Salt and pepper 5%	0.1493	0.2231	0.2623	0.3015	0.2350	0.2822	0.2483	0.3787
	Poisson	0.1832	0.2018	0.2743	0.2477	0.2680	0.2347	0.2480	0.2796
	Gaussian 1%	0.2424	0.2699	0.2620	0.2872	0.2909	0.3035	0.2832	0.2995
r_{fn}	Salt and pepper 5%	0.2447	0.2588	0.2796	0.3926	0.3713	0.3903	0.3810	0.4272
	Poisson	0.2982	0.3068	0.3205	0.3527	0.3893	0.3753	0.3873	0.3836
	Gaussian 1%	0.3690	0.3580	0.3108	0.4262	0.3983	0.4262	0.4255	0.4265

The performance of segmentation algorithms are also compared with respect to a control method, i.e. the one that emerges with the lowest rank. In this study, lowest rank is achieved by the proposed method IIFCM. For comparison of the control method (IIFCM algorithm) with other seven algorithms, we used the post hoc procedure. The post hoc procedure is defined in literature and adjusted p-values are computed in order to find whether the control method is statistically different with the remaining methods. The most widely used post hoc method [38] to obtain adjusted p-values is Holm procedure. Table 9 shows the adjusted p-values for the aforementioned segmentation algorithms corresponding to performance measures ρ, r_{fn} and r_{fp} using Friedman test respectively, where the comparison with control method (IIFCM algorithm) is conducted. The p-values in Table 9 suggest significant difference of the IIFCM algorithm with other algorithms except the IFCM corresponding to ρ and r_{fp}, and FLICM and IFCM algorithms corresponding to r_{fn} at the significance level of 0.05. This shows that the IIFCM algorithm performs significantly better than other segmentation algorithms except IFCM. Similar observation is also made for WM.

5.3. Results on the real brain image corrupted by different noise and comparison of execution time

To check the denoising performance of the proposed IIFCM algorithm with IFCM, FLICM, EnFCM, FGFCM, FCM_S1, FCM_S2 and ImFCM algorithms, we apply these algorithms on the real brain image of size 64×146 pixels corrupted by salt and pepper 5%, Poisson and Gaussian 1% noise. In the experimental setup for brain images corrupted by different noise, we set the value of parameter $\lambda_s (= 3)$, window size 3×3 ($N_R = 8$) [19]. We fixed the fuzzifier constant $m = 2$, number of cluster $c = 4$ and value of $\lambda (= 5.5)$ in IIFCM and IFCM algorithms. Also, we set $\alpha (= 0.2)$ in EnFCM, FCM_S1 and FCM_S2 algorithms after searching optimal value in the interval [0.2, 8] with increment 0.2. The value of parameter λ_g is set to equal to 6 in the FGFCM after searching the optimal value in the interval [0.5, 6] with increment 0.5.

The comparison in the term of similarity index (ρ), false negative ratio (r_{fn}) and false positive ratio (r_{fp}) of all the eight algorithms are shown in Table 10. It can be noted from Table 10 that the similarity index (ρ) of the proposed IIFCM algorithm is more in comparison

Table 11
Comparison of execution time (in seconds) by different segmentation algorithms.

Image type	Image size	IIFCM	IFCM	FLICM	EnFCM	FGFCM	FCM_S1	FCM_S2	ImFCM
Real brain image	64×146	14.51	1.60	21.40	0.27	2.01	97.78	55.10	15.99

to IFCM, FLICM, EnFCM, FGFCM, FCM_S1, FCM_S2 and ImFCM algorithms for salt and pepper 5% noise and Poisson. The segmentation result of the IIFCM algorithm is second best for the Gaussian 1% noise. Also, it can be noted from Table 10, the proposed IIFCM algorithm achieves minimum value of r_{fp} and r_{fn} for all types of noise except the Gaussian 1% noise.

The average execution time of 50 runs of these segmentation algorithms: IIFCM, IFCM, FLICM, EnFCM, FGFCM, FCM_S1, FCM_S2 and ImFCM on real brain image (64×146 pixels) is given in Table 11. It can be observed that the execution time of IIFCM is less than FLICM, FCM_S1, FCM_S2, ImFCM and more than IFCM, EnFCM, FGFCM algorithms. However, the performance of IIFCM is better in comparison to all seven segmentation algorithms in terms of all three measures.

6. Conclusions

In this paper, we have proposed an improved intuitionistic fuzzy c-means (IIFCM) algorithm that overcomes the disadvantage of the IFCM algorithm. The IIFCM algorithm incorporates both local gray-level and spatial information using an intuitionistic fuzzy factor to handle noise and uncertainty during segmentation. It is free of requirement of any parameter tuning. We have performed experiments on synthetic square image, real and simulated MRI brain images, and compared quantitatively their segmentation performance in the term of similarity index, false negative ratio and false positive ratio with seven existing segmentation methods. The obtained results on a synthetic square image and publically available MRI brain images with different noises such as Salt and pepper and Poisson demonstrate the superior performance of the proposed IIFCM algorithm in comparison to existing seven algorithms. Friedman statistical test also show that the proposed IIFCM algorithm performs significantly better than the other algorithms.

Acknowledgments

The authors are thankful to the anonymous reviewers for their constructive suggestions to improve the overall quality of this paper. Moreover, the first author would like to thank the Council of Scientific & Industrial Research (CSIR), New Delhi, India for financial support.

References

[1] Z. Ji, Y. Xia, Q. Sun, Q. Chen, D. Xia, D.D. Feng, Fuzzy local Gaussian mixture model for brain MR image segmentation, IEEE Trans. Inf. Technol. Biomed. 16 (3) (2012) 339–347.
[2] S. Shen, W. Sandham, M. Granat, A. Sterr, MRI fuzzy segmentation of brain tissue using neighborhood attraction with neural-network optimization, IEEE Trans. Inf. Technol. Biomed. 9 (3) (2005) 459–467.
[3] H. Rusinek, M.J. de Leon, A.E. George, L.A. Stylopoulos, R. Chandra, G. Smith, T. Rand, M. Mourino, H. Kowalski, Alzheimer disease: measuring loss of cerebral gray matter with MR imaging, Radiology 178 (1) (1991) 109–114.
[4] K.L. Narr, P.M. Thompson, P. Szeszko, D. Robinson, S. Jang, R.P. Woods, S. Kim, K.M. Hayashi, D. Asunction, A.W. Toga, R.M. Bilder, Regional specificity of hippocampal volume reductions in first-episode schizophrenia, Neuroimage 21 (4) (2004) 1563–1575.
[5] H. Suzuki, J.I. Toriwaki, Automatic segmentation of head MRI images by knowledge guided thresholding, Comput. Med. Imaging Graph. 15 (4) (1991) 233–240.
[6] T. Rohlfing, R. Brandt, R. Menzel, C.R. Maurer, Evaluation of atlas selection strategies for atlas-based image segmentation with application to confocal microscopy images of bee brains, Neuroimage 21 (4) (2004) 1428–1442.
[7] W.E. Reddick, J.O. Glass, E.N. Cook, T.D. Elkin, R.J. Deaton, Automated segmentation and classification of multispectral magnetic resonance images of brain using artificial neural networks, IEEE Trans. Med. Imaging 16 (6) (1997) 911–918.
[8] K. Held, E.R. Kops, B.J. Krause, W.M. Wells, R. Kikinis, H.W. Muller-Gartner, Markov random field segmentation of brain MR images, IEEE Trans. Med. Imaging 16 (6) (1997) 878–886.
[9] C. Li, R. Huang, Z. Ding, J.C. Gatenby, D.N. Metaxas, J.C. Gore, A level set method for image segmentation in the presence of intensity inhomogeneities with application to MRI, IEEE Trans. Image Process. 20 (7) (2011) 2007–2016.
[10] W.M. Wells III, W.E.L. Grimson, R. Kikinis, F.A. Jolesz, Adaptive segmentation of MRI data, IEEE Trans. Med. Imaging 15 (4) (1996) 429–442.
[11] J. MacQueen, Some methods for classification and analysis of multivariate observations, Proceedings of the Fifth Berkeley Symposium on Mathematical Statistics and Probability 1 (14) (1967) 281–297.
[12] J.C. Bezdek, Pattern Recognition with Fuzzy Objective Function Algorithms, Kluwer Academic Publishers, 1981.
[13] Y. Tolias, S.M. Panas, Image segmentation by a fuzzy clustering algorithm using adaptive spatially constrained membership functions, IEEE Trans. Syst. Man Cybern. 28 (3) (1998) 359–369.
[14] D.L. Pham, Spatial models for fuzzy clustering, Comput. Vision Image Underst. 84 (2) (2001) 285–297.
[15] A.W.C. Liew, S.H. Leung, W.H. Lau, Fuzzy image clustering incorporating spatial continuity, IEE Proc. Vis. Image Signal Process. 147 (2) (2000) 185–192.
[16] M.N. Ahmed, S.M. Yamany, N. Mohamed, A.A. Farag, T. Moriarty, A modified fuzzy c-means algorithm for bias field estimation and segmentation of MRI data, IEEE Trans. Med. Imaging 21 (3) (2002) 193–199.
[17] S. Chen, D. Zhang, Robust image segmentation using FCM with spatial constraints based on new kernel-induced distance measure, IEEE Trans. Syst. Man Cybern. 34 (4) (2004) 1907–1916.
[18] L. Szilagyi, Z. Benyo, S.M. Szilagyi, H.S. Adam, MR brain image segmentation using an enhanced fuzzy c-means algorithm, Annu. Int. Conf. IEEE EMB 1 (2003) 724–726.
[19] W. Cai, S. Chen, D. Zhang, Fast and robust fuzzy c-means clustering algorithms incorporating local information for image segmentation, Pattern Recognit. 40 (3) (2007) 825–838.
[20] S. Krinidis, V. Chatzis, A robust fuzzy local information C-means clustering algorithm, IEEE Trans. Image Process. 19 (5) (2010) 1328–1337.
[21] K.T. Atanassov, Intuitionistic fuzzy sets, Fuzzy Sets Syst. 20 (1) (1986) 87–96.
[22] N. Pelekis, D.K. Iakovidis, E.E. Kotsifakos, I. Kopanakis, Fuzzy clustering of intuitionistic fuzzy data, Int. J. Bus. Intell. Data Min. 3 (1) (2008) 45–65.
[23] Z. Xu, J. Wu, Intuitionistic fuzzy c-means clustering algorithms, J. Syst. Eng. Electron. 21 (4) (2010) 580–590.
[24] L.A. Zadeh, Fuzzy sets, Inf. Control 8 (3) (1965) 338–353.
[25] M. Sugeno, Fuzzy Measures and Fuzzy Integrals – A Survey, North-Holland, 1977.
[26] R.R. Yager, On the measure of fuzziness and negation. Part I: Membership in the unit interval, Int. J. Gen. Syst. (1979) 221–229.
[27] R.R. Yager, On the measure of fuzziness and negation. Part II: Lattices, Inf. Control 44 (3) (1979) 236–260.
[28] Z. Xu, Some similarity measures of intuitionistic fuzzy sets and their applications to multiple attribute decision making, Fuzzy Optim. Decis. Mak. 6 (2) (2007) 109–121.
[29] L.K. Hyung, Y.S. Song, K.M. Lee, Similarity measure between fuzzy sets and between elements, Fuzzy Sets Syst. 62 (3) (1994) 291–293.
[30] W.J. Wang, New similarity measures on fuzzy sets and on elements, Fuzzy Sets Syst. 85 (3) (1997) 305–309.
[31] H.W. Liu, New similarity measures between intuitionistic fuzzy sets and between elements, Math. Comput. Modell. 42 (1) (2005) 61–70.
[32] I.K. Vlachos, G.D. Sergiadis, Towards intuitionistic fuzzy image processing, International Conference on CIMCA-IAWTIC (2005) 2–7.
[33] E. Szmidt, J. Kacprzyk, Distances between intuitionistic fuzzy sets, Fuzzy Sets Syst. 114 (3) (2000) 505–518.
[34] A.P. Zijdenbos, B.M. Dawant, Brain segmentation and white matter lesion detection in MR images, Crit. Rev. Biomed. Eng. 22 (5-6) (1994) 401–465.
[35] BrainWeb [online], available: http://www.brainweb.bic.mni.mcgill.ca/brainweb.
[36] Internet Brain Segmentation Repository (IBSR)[online], available: http://www.cma.mgh.harvard.edu/ibsr/.
[37] Brain Extraction Tool (BET) [online], available: http://www.fmrib.ox.ac.uk/fsl/.
[38] J. Derrac, S. García, D. Molina, F. Herrera, A practical tutorial on the use of nonparametric statistical tests as a methodology for comparing evolutionary and swarm intelligence algorithms, Swarm Evol. Comput. 1 (1) (2011) 3–18.
[39] A. Gupta, R.K. Agrawal, B. Kaur, Performance enhancement of mental task classification using EEG signal: a study of multivariate feature selection methods, Soft Comput. (2014) 1–14.
[40] R.L. Iman, J.M. Davenport, Approximations of the critical region of the Friedman statistic, Commun. Stat. Theory Methods 9 (6) (1980) 571–595.